Struct Multidisc Optim 19, 263–273

Optimal structural topologies with transmissible loads

M.B. Fuchs and E. Moses

Abstract In optimal topological design of structures one obtains the configuration of optimal structures when the design domain, the displacement boundary conditions and the applied loads are specified. In the optimal structure one often notices a marked difference between the main bearing structure and the load transfer zones. The latter are composed of relatively light elements the exact nature of which is not always very distinct. The main purpose of this paper is to allow the main bearing part of the structure to emerge. Moreover the actual location of the load along its line of action is not always a design requirement. In order to include this relaxed condition regarding the loading position the concept of transmissible or sliding forces is introduced in topological design of structures. A transmissible force is a force of given magnitude and direction which can be applied at any point along the line of action of the force. The optimization formulation is similar to standard topological design procedure in addition to the condition of transmissability of the forces. It is shown that this condition reduces to an equal displacement constraint along the line of action of the forces. The method is illustrated by typical structural examples. It is observed that this numerical method produces indeed crisp images of the main structural components, unblurred by the secondary load transfer elements. It is also indicated that many results are often replicas of Prager structures which were previously obtained by analytical methods.

Key words transmissible loads, topology optimization, Prager structures, compliance design

Received March 3, 1999

M.B. Fuchs and E. Moses

Department of Solid Mechanics, Materials and Structures, The Iby and Aladar Fleischman Faculty of Engineering, Tel Aviv University, 69978, Tel Aviv, Israel
e-mail: fuchs@eng.tau.ac.il,
http://www.eng.tau.ac.il/~fuchs

1 Introduction

With the exception of a few early landmark results (Maxwell 1890; Michell 1904) the historical development of the field of structural optimization (Haftka *et al.* 1990; Kirsch 1993) seems to have followed an opposite route to the actual structural design process. Since its inception, research in numerical optimal structural design went from element stiffnesses design, through geometric and shape optimization to topological design. In a proper sequence the topological and shape designs come first and then one can finalize the structure by determining its cross-sectional characteristics. It is also clear that the major impact on the structural efficiency, in the sense of stiffness/volume or stress/volume ratios, is determined at the conceptual state by the topology and shape of the structure. No amount of fine tuning of the cross-sections and thicknesses of the elements will compensate for a conceptual error in the topology or the structural shape (see for instance Olhoff *et al.* 1991).

It is only natural that with the proliferation of cheaper computing power research was rightly channeled to shape and topology optimization as can be seen in the review papers of Haftka and Gandhi (1986), Kirsch (1989) and Rozvany *et al.* (1995). A numerical approach to topological design starts with a domain of material to which the external loads and support conditions are applied. The initial domain is homogeneous at the macroscopical scale, a condition which precludes any preferential or intuitive design concepts. The optimization algorithm then proceeds with carving out ineffectual material in order to generate best structural solutions. Auster (1988, p. 132) in describing Michaelangelo's notion of sculpture paraphrases the concept: "the figure is already there in the material; the artist merely hews away at the excess matter until the true form is revealed."

The objective function is often the compliance (Taylor 1977), that is, the flexibility of the structure under the given loads, subject to a volume of material constraint. Two classes of structural domains have been used. In a first instance one considers a trussed structure com-

posed of a densely packed set of nodes and axial elements which connect all (or most) pairs of nodes. This is called the "ground" structure and the premise is that the optimal configuration can be found in the plethora of trusses embedded in the ground structure. Early solutions can be seen in the papers of Dorn *et al.* (1964) and Dobbs and Felton (1969). Examples of applying the concept to large-scale structures were presented, for instance, by Zhou and Rozvany (1991). The other class of structural domains is a continuous sheet of material in 2D or a block of material for 3D structures. The continuum is typically divided into appropriate finite elements where every element has intrinsic structural properties.

In the "relaxed" formulation (Allaire and Kohn 1993) we assume that the material in every element consists of perforated periodic microstructures. In these composite materials the inclusion is a low stiffness material, representing the void inclusions, and the matrix is made of the basic material of the structure. As noted by Olhoff *et al.* (1997) the microstructure should allow for the entire range of densities, and be periodic in order to allow to compute effective material properties. The design variables of the optimization problem are the densities of the elements. By setting the densities of elements to zero or to one the algorithm removes ineffective material from the design while keeping structural important regions. The formal statement of the problem is

$$\min_{\rho} \left\{ \int_V u_m(\rho) b_m \, \mathrm{d}V + \int_S u_m(\rho) t_m \, \mathrm{d}S | \int_V \rho \, \mathrm{d}V = \rho_o V \right\}$$

$$(\text{summation over } m) \,, \tag{1}$$

where ρ is the local density function, u_m, b_m and t_m are the components of the displacements, body forces and surface tractions, respectively, ρ_o is an initial uniform density and V is the volume of the design domain. At this state the ρ function is to be construed as a generic quantity implying the type of local composite and amount of material. In this raw form the problem statement is rather simple but finding the optimum is not a trivial affair.

A major contribution to the solution of (1) was made by Bendsøe and Kikuchi (1988) by formulating the problem through a finite element representation and by restricting the relaxed formulation to composites with repetitive rectangular holes (Suzuki and Kikuchi 1991; see also Diaz and Bendsøe 1992). The design variables for every element were the density ρ and the angular orientation θ of the orthotropic material with respect to the system axis. What ignited the interest in this approach is that we had now a method for designing the topology (and shape) of a structure with almost no specifications other than the location of the loading and the supports. This was in sharp contrast to previous work in optimization where the general layout of the final structure was fixed *a priori*. And indeed, much progress has been made with these new techniques and many interesting structural instances have been produced.

One will note that there are several ingredients to the method incepted by Bendsøe and Kikuchi (1988). First and foremost is the finite element representation of the design domain, and the assumption that in every element i we have a material whose density is a design variable. In addition an orthotropic composite with repetitive rectangular voids with a density ρ_i and and a material orientation θ_i where used. Other orthotropic materials can also be employed, such as rank-2 optimal composites (Allaire and Kohn 1993; Gibiansky and Cherkaev 1984; Vigdergauz 1986). In some works we find "Solid Isotropic Microstructure with Penalty" or SIMP material (Rozvany *et al.* 1992) of the form

$$E = E_o \rho^{\eta_1} \,. \tag{2}$$

Here E_o is the modulus of the material and η_1 is an arbitrary parameter. This artificial modulus can be tuned in order to produce 0/1 (material/void) type solutions thus generating crisp structural topologies.

The second ingredient is the objective function. It so happens that the success of the method hinges on the finite element and material modeling but not on the use of specific objective function. One could very well consider an "engineering" optimality criterion method for topological design. Instead of basing the iterations on the mathematical criteria that a design must fulfill at the minimum, the structure is modified by removing understressed material and by adding material in highly stressed regions thus yielding fully-stressed designs. It was an early attempt for designing structures, based on the premise that if the material is properly used, the design can not be all that bad. Although shielded by mathematical programming methods and more so by optimality criteria based on the Kuhn-Tucker conditions at a local minimum, the stress-ratio has retained its popularity. It has now found its way into topology design class of problems as in the papers by Hinton and Sienz (1995) and Fuchs *et al.* (1999) and in the Hard Kill method as in that of Van Keulen and Hinton (1996). Examples can also be found in the papers by Mattheck and Burkhardt (1990), Xie and Steven (1997) and Tanaka *et al.* (1995) where the iterative procedure mimics the stress induced growth of bone and plant material. All these techniques are in fact variations on the classic stress-ratio theme. The popularity of this iterative approach rests on the premise that it usually generates very sound engineering structures. For instance, it is widely accepted that the uniform stress condition is most probably the criterion which determines the adaptation of bones in humans and other mammals. Indeed, bone throughout the life-time of the individual is responding to the conditions under which it is being used (Beaupre *et al.* 1990; Lanyon 1987).

Citing from Beaupre we note that if bone tissue experiences excess stimulation, additional bone will be deposited. If bone tissue experiences insufficient stimulation, it will resorb.

In this paper we propose to further relax the design problem by allowing the external loads to move along their line of action. In other words, we have a set of loads to be supported by the structure but we do not specify the exact location of the points of application of the loads. In fact what we are seeking is not only the optimal topology for a set of loads and supports but also the optimal point of application of the loads. A simple example will illustrate the concept. Consider the problem of designing a symmetric structure to support a force at two hinged supports as shown in Fig. 1. It is clear that when the load position is prescribed, as in Fig. 1a the optimal topology and geometry depends on that position of the force. We are interested in case Fig. 1b where we seek to design a structure for a force without specifying its point(s) of application. Only the line of action of the force is imposed. The answer will indicate where the structure would like the force to be in order to optimize the objective function. In this simple example the optimal topology for minimum compliance under a constant volume constraint (the cross-sectional areas can vary) can be shown to be an isocele truss with 45° sloping members as in Fig. 1c.

The concept of movable loads is structural optimization is not new. It appears in the definition of Prager structures (see Rozvany and Prager 1979). Prager structures are stress-constrained least-weight trusses where the sign of the member stresses must be the same in all elements and the loads are allowed to move along their line of action. The structure in Fig. 1c is in fact a Prager truss (Rozvany *et al.* 1982) for the moving load and hinged supports.

By using transmissible loads in a topological context we are isolating the design of the main load bearing part of the structure from the design of the secondary load transfer problem. An arch-bridge for instance is composed of the actual arch which transfers the load to the reactions, a deck to which the load are applied and local load transfer elements which connect the deck to the arch. For a lower deck these elements are in tension and could for instance be cables in tension. With an upper deck we will have struts in compression. By using the present approach we will be designing the arch only, leaving the secondary load tranfer elements for a later stage.

In the following section we will describe the general guidelines for a topological design of structures, in particular for the design of minimum compliance solutions under constant volume of material. Next we will adapt these techniques for the case of sliding loads. A subsequent section will illustrate the approach with selected typical examples. Finally, a concluding section will close this work and indicate possible directions for future work on the subject.

2
Standard topological optimization

We will review the main steps of a standard method for topological design of minimum compliance (1). One starts from a design domain (region where material can be located) to which external loads are applied and where displacements boundary conditions are specified. The domain is meshed into finite elements and every element is made of a porous isotropic or orthotropic material. The design variables are the densities $\boldsymbol{\rho}$ which determine the material properties of the elements. In the following we will assume that the material is isotropic (2) and that $\boldsymbol{\rho}$ is the design vector. The analysis of the structure is relaxed by requiring that at the optimum the total potential functional be minimized with respect to the nodal displacements. And since at that minimum the total potential is equal to minus the strain energy (twice the compliance), problem (1) can now be stated as

$$\max_{\boldsymbol{\rho}} \min_{\mathbf{u}} \left\{ (\mathbf{u}'\mathbf{K}\mathbf{u} - \mathbf{p}'\mathbf{u}) | \sum_j \rho_j V_j = \rho_o V \right\}, \tag{3}$$

where $\mathbf{u}$ is the nodal displacements vector, $\mathbf{p}$ is the applied loads vector, $\mathbf{K}$ is the stiffness matrix of the structure, ρ_j is the material density in element j, V_j is the volume (area times constant thickness) of element j, index j runs over all the finite elements, and $(.)'$ is the matrix transpose operator. It will be noted that the value of $0 \leq \rho_o \leq 1$ controls the amount of material available for the design.

One can now build a Lagrangian function

$$L(\boldsymbol{\rho}, \lambda, \mathbf{u}) = (\mathbf{u}'\mathbf{K}\mathbf{u} - \mathbf{p}'\mathbf{u}) - \lambda(\rho_j V_j - \rho_o V), \tag{4}$$

where $\mathbf{K}(\boldsymbol{\rho}) = \sum_j \mathbf{K}_j(\rho_j)$ and $\mathbf{K}_j$ is the stiffness matrix of element j in global coordinates. Equating the derivatives of L with respect to ρ_j, λ and $\mathbf{u}$ to zero yields, respectively,

$$\mathbf{u}' \frac{\partial \mathbf{K}_j}{\partial \rho_j} \mathbf{u} - \lambda V_j = 0, \quad j \in J, \tag{5}$$

$$\sum_j \rho_j V_j - \rho_o V = 0, \tag{6}$$

$$\mathbf{K}\mathbf{u} - \mathbf{p} = 0. \tag{7}$$

Equations (5) and (6) form the basis for the minimization iterations. The last equation (7) will automatically be satisfied since we will be using the actual displacements for the iterations. Equation (5) produces the optimality condition for minimum compliance

$$1 = \frac{\left(\mathbf{u}' \frac{\partial \mathbf{K}_j}{\partial \rho_j} \mathbf{u}\right) / V_j}{\lambda}. \tag{8}$$

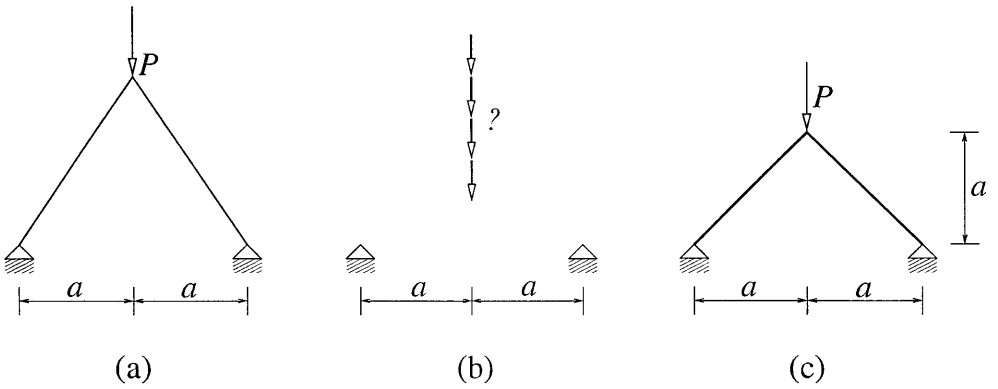

Fig. 1 Optimal topologies for central load on two hinged supports: (a) The design depends on the point of application of the load, (b) What is the optimal design for a transmissible load? (c) Optimal solution for minimum compliance of a transmissible load under a constant volume constraint

Since λ is a constant the optimality condition states that at the minimum the quantity $(\mathbf{u}'\partial\mathbf{K}_j/\partial\rho_j\mathbf{u})/V_j$ is a constant. When multiplying both sides of (8) by ρ_j (a common practice with optimality conditions) one generates the iterations formula

$$\rho_j^{(k+1)} = \left[\rho_j \frac{\left(\mathbf{u}'\frac{\partial\mathbf{K}_j}{\partial\rho_j}\mathbf{u}\right)/V_j}{\lambda}\right]^{(k)}, \tag{9}$$

where k is the iterations index.

Very similar equations can be developed by using a stress-ratio method for generating fully stressed designs (FSD)

$$1 = \frac{\sigma_j}{\overline{\sigma}}, \tag{10}$$

where σ_j is a representative stress for element j, usually the von Mises effective stress, and $\overline{\sigma}$ is a target stress. As such it is a measure of the strain energy of distortion $U_d = \sigma_e^2/6G$, where G is the shear modulus. The two quantities, $(\mathbf{u}'\partial\mathbf{K}_j/\partial\rho_j\mathbf{u})/V_j$ and σ_j, although not equal are nevertheless of a similar structural significance. After multiplying both sides by the density we obtain the classical stress-ratio iterations

$$\rho_j^{(k+1)} = \left(\rho_j \frac{\sigma_j}{\overline{\sigma}}\right)^{(k)}. \tag{11}$$

The introduction of ρ_j in both sides of (8) and (10) is crucial in the topology context. It sets up the iterations on ρ_j, but more so it allows for solutions $\rho_j = 0$, which is the essence of topology design. Thus, if condition (8) or (10) can be enforced, element j remains in the design. If not, then the element is removed.

In both iterative procedures we have an undefined constant (λ in the compliance iterations and $\overline{\sigma}$ in the FSD case). The classical way to deal with these loose parameters differs in the compliance and in the FSD approach. In the former, (9) is introduced in the constant volume condition (6) to yield the final form of the iterations for minimum compliance

$$\rho_j^{(k+1)} = \rho_o \frac{V}{V_j}\left(\frac{\rho_j \mathbf{u}'\frac{\partial\mathbf{K}_j}{\partial\rho_j}\mathbf{u}}{\sum_j \rho_j \mathbf{u}'\frac{\partial\mathbf{K}_j}{\partial\rho_j}\mathbf{u}}\right)^{(k)}. \tag{12}$$

In the stress-ratio iterations the target stress $\overline{\sigma}$ is typically the largest allowable stress. Since ρ cannot exceed 1, $\overline{\sigma}$ was selected by Fuchs *et al.* (1999) as

$$\overline{\sigma} = \max_j\{\sigma_j\}. \tag{13}$$

Consequently the densities are automatically confined within the 0/1 bounds. In the case of multiple loading conditions one usually replaces the compliance by a weighted sum of compliances as objective function

$$\max_{\boldsymbol{\rho}} \min_{\mathbf{u}} \left\{\sum_{\ell=1}^{n_\ell} w_\ell(\mathbf{u}_\ell'\mathbf{K}\mathbf{u}_\ell - \mathbf{p}'\mathbf{u}_\ell) \middle| \sum_j \rho_j V_j \le \rho_o V\right\}, \tag{14}$$

where w_ℓ is a weighting factor for load condition ℓ and n_ℓ is the number of loading conditions. With FSD the accepted method is to define the representative stress as the highest among all loading conditions

$$\sigma_j = \max_\ell\{\sigma_{j\ell}\}, \tag{15}$$

where $\sigma_{j\ell}$ is the representative stress in element j for load condition ℓ. There is one more important ingredient. The densities must remain within the bounds $0 \le \rho_j \le 1$. Consequently iterations (12) are supplemented with

$$\begin{aligned} &\text{if} \quad \rho_j < 0 \quad \text{then} \quad \rho_j = 0, \\ &\text{if} \quad \rho_j > 1 \quad \text{then} \quad \rho_j = 1. \end{aligned} \tag{16}$$

This requires of course an inner loop on the densities in order to fulfill the constant volume constraint.

These are the basic forms of the minimum compliance iterations with a constant volume constraint and the FSD iterations with a maximum target stress condition.

3
Typical results using the standard approach

Consider the design of a structure to support a distributed uniform load on two hinged supports (Fig. 2). The reactions are at the lower corners of a rectangular design domain and two cases are considered: the distributed load acts (a) along the lower boundary, and (b) along the upper boundary. The material in every element j is isotropic, the design variables are the densities ρ_j in every element, Poisson's ratio is $\nu = 0.3$ and Young's modulus is given by (2) where E_o is an arbitrary constant with $\eta_1 = 1.5$.

Note, the element stiffness matrix in global coordinates is $\rho_j^{\eta_1}\hat{\mathbf{K}}_j$ where $\hat{\mathbf{K}}_j$ is the element stiffness matrix with Young's modulus E_o. Consequently, the derivative in (12) is simply $\eta_1\rho_j^{\eta_1}\hat{\mathbf{K}}_j$ and (12) becomes

$$\rho_j^{(k+1)} = \rho_o \frac{V}{V_j}\left(\frac{\rho_j^{\eta_1}\mathbf{u}'\hat{\mathbf{K}}_j\mathbf{u}}{\sum_j \rho_j^{\eta_1}\mathbf{u}'\hat{\mathbf{K}}_j\mathbf{u}}\right)^{(k)} . \tag{17}$$

Iterations (17) were used with a total amount of material $\rho_o = 0.2$, $V_j = 1$ and $V = 24 \times 48 = 1152$ finite elements. Unless specified to the contrary 4-node PLANE42 bilinear isoparametric (Ansys Swanson Analysis Systems, Inc. (1992)) elements were employed. The configurations after convergence are shown in Fig. 3. We should like to draw attention to the two distinct parts of the design. There is first the arch which is the actual load-bearing structure. It is characterized by a concentration of matter. Next there are the secondary structural components which transfer locally the applied loads to the arch. These are lightweight zones which may represent in case (a) a cable network to transfer the tension forces and in (b) a set of struts. One notes that both loadings call for an arch but the primary structure differs in both cases. In other words, by deciding on the location of the loads one influences the final design of the primary structure. Al-

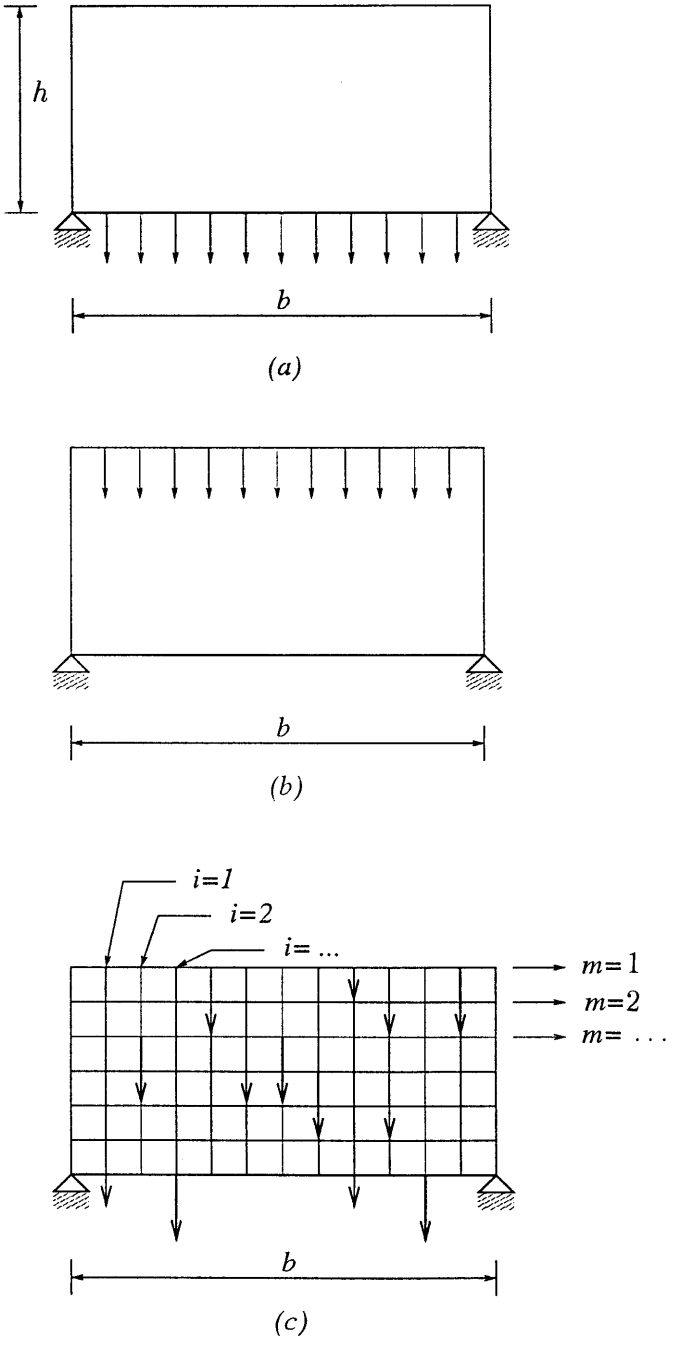

Fig. 2 Design domain on two hinged supports for supporting a distributed load on (a) upper boundary, (b) lower boundary and (c) with transmissible loads

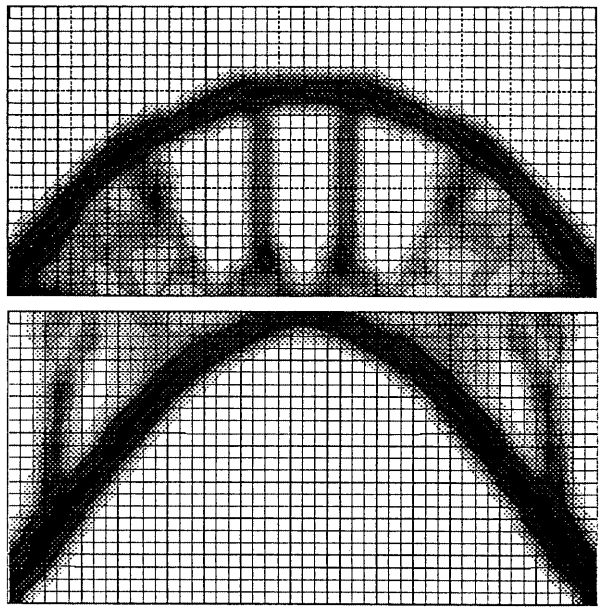

Fig. 3 Optimal topologies for a distributed fixed load on two hinged supports with the load applied (a) to the upper boundary and (b) to the lower boundary. Note the distinct primary structure (black) and the secondary (grey) load transfer parts

though there is much to learn from the layouts of the secondary structures we should like to concentrate on the "pure" design of the primary structure, the arch in this example. That is, if we let the equations find best positions of the applied loads, what would the optimal primary structure be?

For this purpose we introduce transmissible loads or sliding loads as in Fig. 2c. The graphic rendering of the applied loads indicates that the exact location of the applied forces is also a variable of the design. What is given is the magnitude and the line of action of the forces. Moreover, the design stipulation allows for the splitting of a load into several forces along the same line of action while keeping the total magnitude constant. An outline for the inclusion of transmissible structures is given in the next section.

4
Topology design with transmissible loads

In this section we will essentially retrace the method of the standard approach while making allowance for transmissible forces. For the sake of clarity we restrict the formulation to transmissible forces which are aligned with a subset of degrees of freedom in global coordinates, as in example Fig. 2c. The theory remains valid for forces which are transmissible along other directions since one can always remesh the domain to make the lines of action coincide with global degrees of freedom.

An example of transmissible forces can be seen in Fig. 2c where vertical loads act along lines of action $i \in I$. Within each group i the applied force p_i can can be split into p_{im}s, $m \in M$, with the equality constraints

$$\sum_{m\in M} p_{im} - p_i = 0\,, \quad i \in I\,, \tag{18}$$

where M is the number of nodes along every line of action. In the particular case of Fig. 2c we have $I = 11$ transmissible vertical loads where every load can be distributed amongst $M = 7$ nodes. The task of the design is thus to position these loads in an optimal fashion in conjunction with a topological design of the structure. The compliance minimization problem (3) is now

$$\max_{\rho}\ \max_{p_{im}}\ \min_{\mathbf{u}} \Big\{ (\mathbf{u}'\mathbf{K}\mathbf{u} - \mathbf{p}'\mathbf{u}) |\quad \sum_j \rho_j V_j = \rho_o V\,;\quad \sum_{m\in M} p_{im} - p_i = 0\,, \quad i \in I \Big\}\,. \tag{19}$$

This leads to the Lagrangian function

$$L(\boldsymbol{\rho}, \lambda, \mathbf{u}, p_{im}, \mu_i) = (\mathbf{u}'\mathbf{K}\mathbf{u} - \mathbf{p}'\mathbf{u}) - \lambda(\rho_j V_j - \rho_o V) - \sum_{i\in I} \mu_i \Big(\sum_{m\in M} p_{im} - p_i \Big)\,. \tag{20}$$

Equating the derivatives of $L(\boldsymbol{\rho}, \lambda, \mathbf{u}, p_{im}, \mu_i)$ with respect to the variables to zero gives respectively (5), (6) and (7) with the addition of

$$u_{im} - \mu_i = 0\,, \quad i \in I\,, \tag{21}$$

and (18). Here u_{im} are the displacements corresponding to p_{im}. The new information is in (21). We find that with sliding loads the displacements along the lines of action of the p_i are constant, $u_{im} = \mu_i$. This was to be expected. In order to design a structure where the position of the load along the line of action is immaterial one could assume the existence of infinitely stiff axial elements of zero mass along that line. This also makes the displacements constant along the line.

An alternative way of looking at the problem is to introduce the sliding loads condition directly into the equilibrium equations (7). Indeed, let $\mathbf{p}_i$ be the external loads vector along line of action i. The condition of transmissability (18) can also be written as

$$p_i = \mathbf{b}'\,\mathbf{p}_i\,, \tag{22}$$

where $\mathbf{b}$ is 1-valued vector. Using this type of relation for all the sliding forces in a load transformation equation

$$\overline{\mathbf{p}} = \boldsymbol{\Gamma}'\mathbf{p}$$

leads to the reduced equilibrium equations

$$(\boldsymbol{\Gamma}'\mathbf{K}\boldsymbol{\Gamma})\overline{\mathbf{u}} = \overline{\mathbf{p}}\,, \tag{23}$$

with

$$\mathbf{u} = \boldsymbol{\Gamma}\overline{\mathbf{u}}\,.$$

In this equation the line corresponding to (22) is

$$\mathbf{u}_i = \mathbf{b}\,u_i\,, \tag{24}$$

where u_i, or μ_i in (21), is the common displacement of the line of action i.

It will be noted that the only difference between the design for fixed loads and the design for sliding loads is that in the latter the analysis equations (7) are replaced by (23). Consequently what has been developed for minimum compliance under a constant volume constraint remains valid for an FSD design (11) as long as the analysis is performed with the congruent transformation in (23).

5
Numerical examples

As an introductory example we will solve the minimum compliance problem with constant volume of material for a transmissible load symmetrically reacted by two hinged supports. The design domain is the ground structure used by Rozvany *et al.* (1982). It is composed of densely spaced isocele two-bar trusses with apex along the line of action

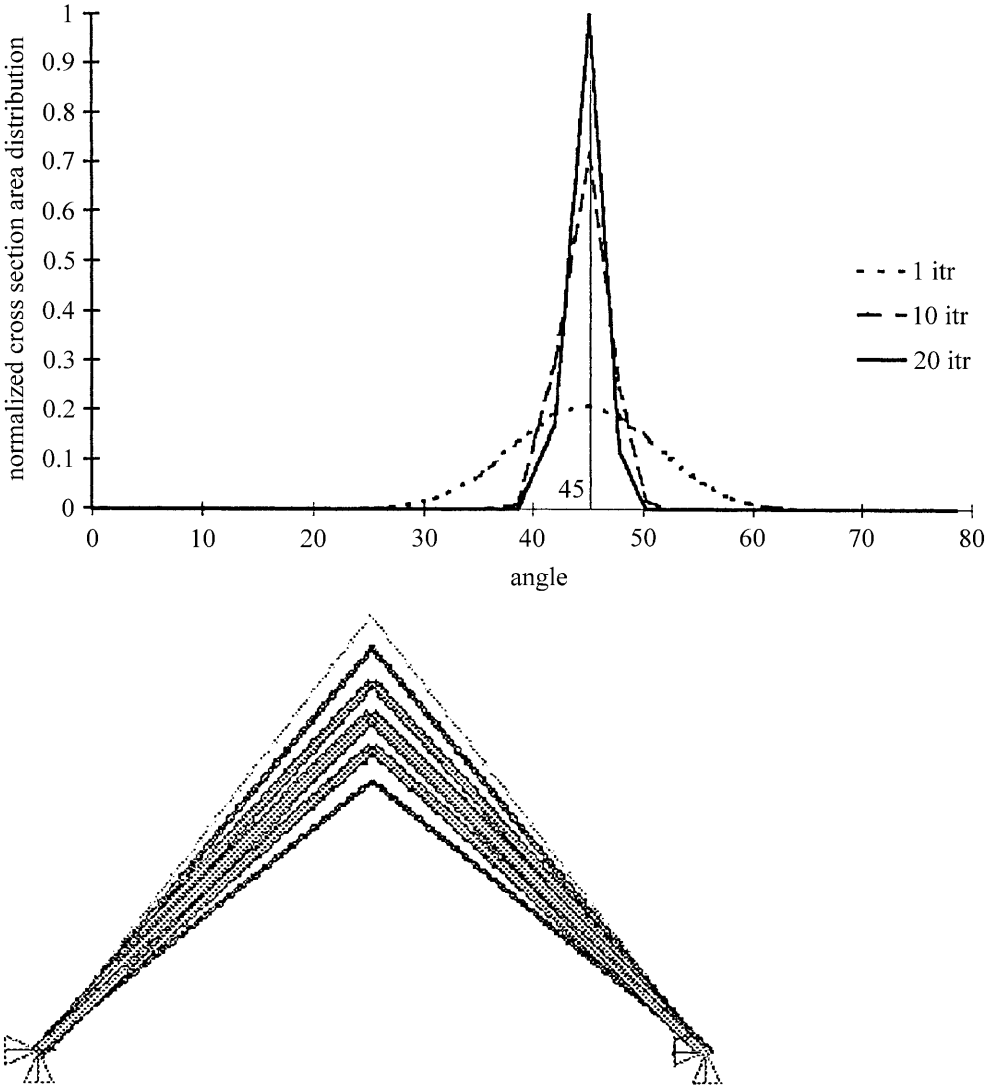

Fig. 4 Convergence history and intermediate topology for a point mid-way between two hinged supports. The graph gives the cross-sectional areas distribution as a function of the bar slope after 1, 10 and 20 iterations. The figure at the bottom shows an intermediate solution

of the load and the design variables are the cross-sectional areas of the bars. In the context of sliding loads we have also an infinitely stiff element of zero mass along the line of action of the force. An intermediate design is shown in the right of Fig. 4. Clearly, the axial stiffnesses of the elements pile up along members close to the 45° line. As noted earlier the optimum solution is a 45° truss. In the left graph of Fig. 4 we show the convergence history of the iterative scheme. The figure depicts the distribution of the cross-sectional areas as a function of the slope of the elements after 1, 10 and 20 iterations. One notices the spread of material about the dominant 45° angle element.

We now turn our attention to the solution of the same problem using a continuous domain (Fig. 1b) and also to the solution of a similar problem for sliding distributed loads acting perpendicular to the line connecting two hinged supports (Fig. 2c). The design domains in Fig. 5 are rectangles of aspect ratios (bottom to top) 0.25, 0.40 and 1.00 and the corresponding volume fractions are 0.1, 0.1 and 0.2. The material is isotropic with an elastic modulus given by (2) and Poisson's ratio $\nu = 0.3$. The domain is redesigned with the use of (12) in conjunction with a tuning parameter η_2.

$$\rho_j \leftarrow \rho_o \frac{V}{V_j} \left(\frac{\rho_j \mathbf{u}' \frac{\partial \mathbf{K}_j}{\partial \rho_j} \mathbf{u}}{\sum_j \rho_j \mathbf{u}' \frac{\partial \mathbf{K}_j}{\partial \rho_j} \mathbf{u}} \right)^{\eta_2} . \tag{25}$$

Parameter η_2 is employed for improving the convergence.

The results are shown in Fig. 5 (left) for the single load and (right) for the distributed load. The reason for selecting different aspect ratios for the design domain is to compare cases which have to deal with restricted design domains (aspect ratios 0.25, 0.40) with a "free" design example (aspect ratio 1.00). In the case of the point load we obtain for the lowest aspect ratio a solution were the applied load is split in two parts were the bottom load

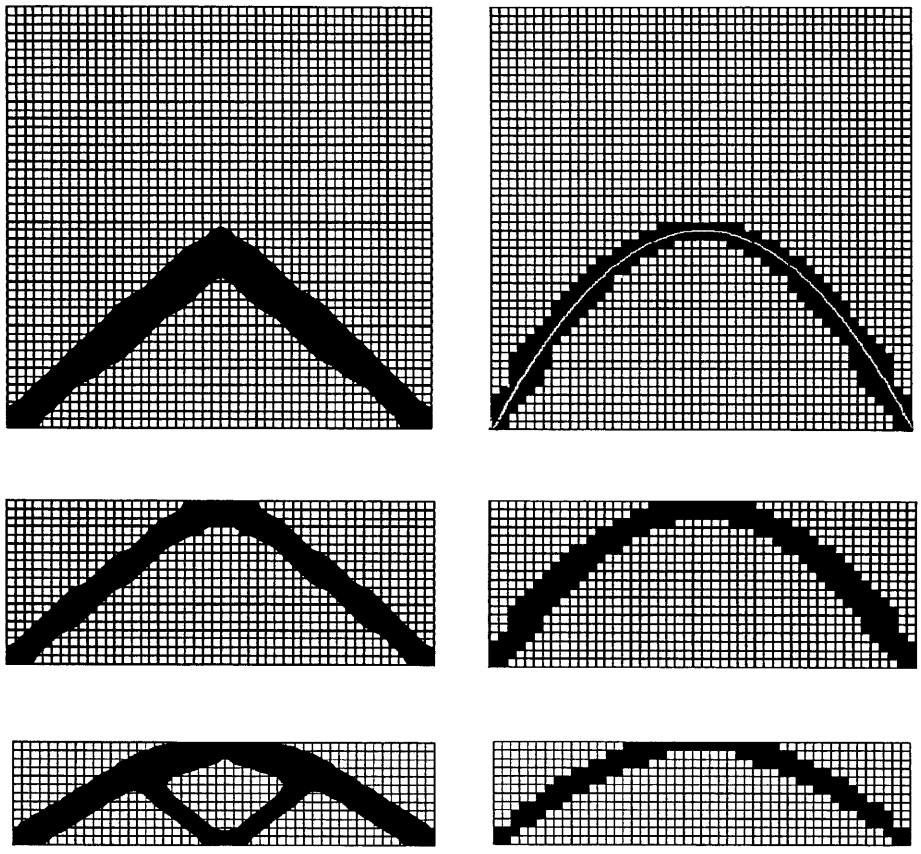

Fig. 5 Optimal topologies for supporting (left) a transmissible force and (right) a transmissible distributed load on two hinged supports, as a function of the design domain aspect ratios 0,25, 0.40, and 1.00. In the lower figure 0.65 of the load is taken by the upper part and 0.35 by the lower part

is connected by tension ties to a pseudo-arch in compression. We note that the upper portion takes 0.65 of the load and the lower tension rods the remaining 0.35. With higher aspect ratios we obtain isocele truss solutions. In the free design domain the optimal solution is the 45° Prager structure. For the distributed load cases (right) we have in all instances parabolic-type arch structures. In the case of the free design domain we have superimposed on the arch a parabola originating at the crown and passing through the hinged supports. The fit is almost perfect. The height-to-base ratio of this parabola is $h/b = 0.479$. We have also checked analytically the optimal height of a minimum compliance parabolic arch under a uniform distributed load with a constant volume constraint. The design variables were the continuous distribution function of cross-sectional area and h/b. It was found that the minimal solution has a constant stress and the optimal height is $(h/b)_{\min} = \sqrt{3}/4 = 0.433$ which is a little less that what is shown in Fig. 5. Incidently, $\sqrt{3}/4$ is also the height of the optimal Prager arch (Rozvany and Wang 1983).

It is worthwhile to compare the optimal solution with sliding distributed forces to the ones with fixed forces in Fig. 3. We have already mentioned that in the fixed forces cases the solution includes both the load bearing part (the arch) and the secondary local load transfer zones. Using sliding loads produces the optimal load carrying structure only. The designer can then decide if the optimal location of the applied loads suits the environmental requirements or not. In the negative he can add proper load transfer parts to the structure. The important issue is that with sliding forces we obtain both the stiffest structure and the optimal locations for applying the forces. It should be recognized that with sliding loads the compliance was found to be 0.506 as compared to 1.09 and 1.04 for the left and right cases in Fig. 3. The numbers are expressed relative to some datum structure.

Finally, with regard to the graphic rendering of the results in Fig. 5, the arches were left in their discretized configuration and are built-up from square finite elements whereas the trusses to the left were smoothened out by an interpolation technique.

With regard to the η_1 parameter in the constitutive law (2) and η_2 in (25) the reader is referred to Fig. 6. Here we have depicted typical intermediate solutions obtained during the optimization of the distributed load case. Moving anti-clockwise from the left lower figure we show designs after 1, 3, 9 and 12 iterations. We notice a tendency for a double arch solution where the primary structure seems to carry a secondary one. It is however clear that the upper arch is the result of stress increases at the upper domain boundary. In order to clean up the picture the

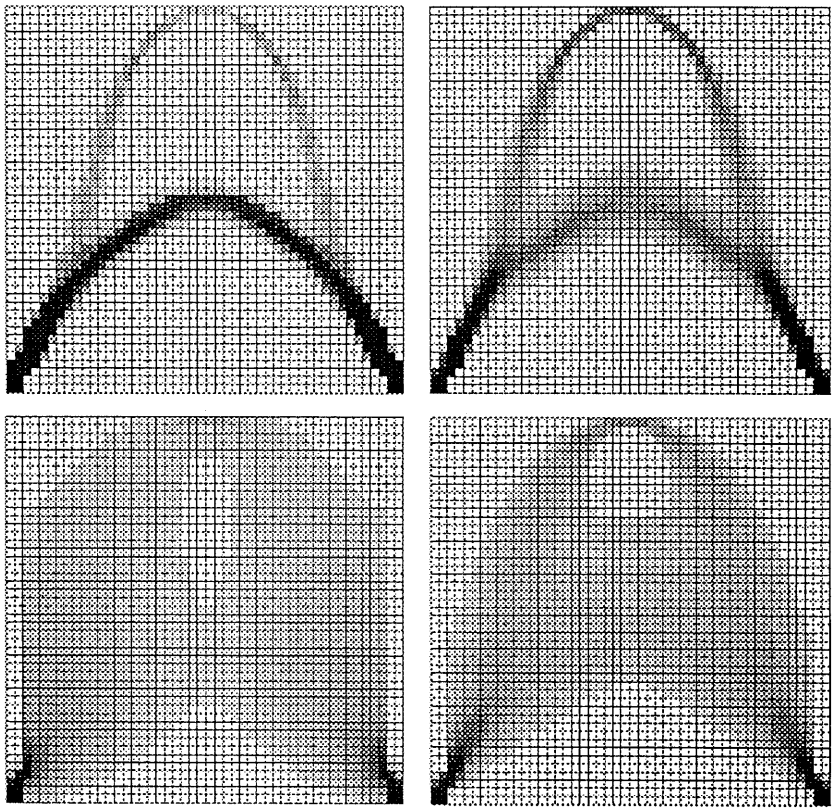

Fig. 6 Intermediate steps of the parabolic arch design in Fig. 5. From left corner anti-clockwise at 1, 3, 9, 12 iterations. The upper arm is due to boundary induced stress concentrations and is gradually eliminated by incrementing η_1, the dependence of Young's modulus upon the density (2), from 0.5 to 2.0

material parameter η_1 was iteratively increased

$$\eta_1^{(k+1)} = \eta_1^{(k)} + \Delta\eta_1 \,, \tag{26}$$

with $\eta_1^{(0)} = 0.5$ and $\Delta\eta_1 = 0.075$. The second parameter was kept constant at $\eta_2 = 0.8$. Although other numerical schemes are possible, it seems that initially, when the design domain is almost homogeneous, values $\eta_1 < 1$ should be used. Indeed, they modify the stiffness moderately and allow the procedure to produce the fundamental patterns. Gradually, the increasing values of η_1 help the design in eliminating "noise" and in retaining the optimal topology.

The effectiveness of employing sliding loads in topology design is perhaps best emphasized in the design of a 3D structure to support a uniform distributed load normal to a square plane and supported at the 4 corners of the plane. The initial design domain was a rectangular parallelepiped loaded and supported as shown in Fig. 7, the grey domain representing the uniform load. The material volume was $\rho_o = 0.1$. Using a $17 \times 17 \times 17$ mesh (quarter domain), with 8-node SOLID45 isoparametric elements, lower and upper views of the resulting design can be seen in Figs. 8 and 9, respectively. The structure is reminiscent of the two-way vaulting of Gothic structures. The material densities of all the retained elements is equal to 1, the shades of grey indicating elevation. We have here

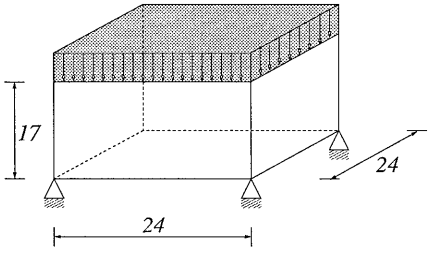

Fig. 7 Design domain for uniform distributed sliding loads normal to a square area and supported on four supports at the corners

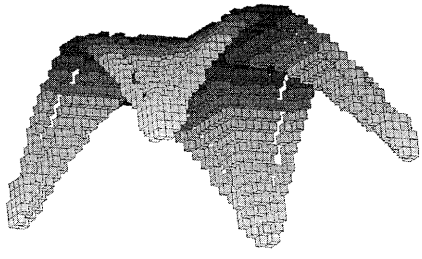

Fig. 8 A 3D example. Starting from a $10 \times 10 \times 10$ block of material supported at the 4 corners and submitted to sliding distributed loads normal to the ground the optimal solution is reminiscent of a Gothic vaulting. This result was obtained for a $\rho_0 = 0.1$. Note, all elements have a density of 1, the shades of grey indicate elevation

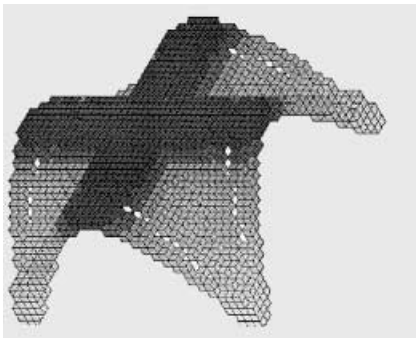

Fig. 9 Structure in Fig. 8 viewed from above

a series of 4 arches over the adjacent supports and two arch vaults over diagonal supports. The highest level of material, shown in a dark shade, is a cross supported at the crowns of all 6 arches. One will notice discontinuities running parallel to the side arches. What appears to be voids are simply regions with large variation of the elevation. Assumably these "windows" should disappear when using a higher density mesh. Here also (26), $\eta_1^{(0)} = 0.5$, $\Delta\eta_1 = 0.075$ and $\eta_2 = 0.8$.

6 Conclusions

This paper is concerned with the optimum topological design of structures subjected to transmissible forces. The term refers to loads for which the line of action is given but the exact location(s) of the forces along the lines of action is part of the optimization process. This allows a further relaxation of the topology design problem. Indeed, the layout of the optimum topology structure depends heavily on the location of the applied forces. Since the fundamental premise of topological design is to produce results which are independent on some preassumed concepts, fixing the applied forces constitutes an infringement on this principle. Whenever possible, the forces should be allowed to move along their line of action. This has also the merit of generating the pure structural part of the solution uncluttered by local force transmission elements. In simple cases the procedure often produces Prager trusses which are composed of uniformly stressed structures of same sign. The method can however be extended to more complex situations.

It is shown that using transmissible forces is equivalent to assuming equal displacements along the line of action. Alternatively, the structure can be considered to be embedded with infinitely stiff axial members of zero mass, along every applied force line. This is a relatively simple algorithmic requirement and can easily be incorporated in FE analysis routines. The numerical technique converges rather smoothly once the method for eliminating parasitical parts has been mastered. Indeed, the interaction of the infinitely stiff elements with the boundaries of the design domain may cause stress increases which have a tendency to draw material. It is shown how a judicial change of the stiffness-density relations during the minimization can eliminate the unwanted portions of the structure thus paving the way for the optimal solution. Possible further extensions of the concept of transmissible loads is the topological design of structure under pressure loads where the external forces are limited to the external boundary of the material, follow its modifications and are constrained to act normal to the loaded boundary (Hammer and Olhoff 1999). This could be used in the design of the dams for instance. Some work along these lines is presently being pursued.

References

Allaire, G.; Kohn, R.V. 1993: Optimum design for minimum weight and compliance in plane stress using extremal microstructures. *Eur. J. Mech., A/Solids* **12**, 839–878

Auster, P. 1988: *The invention of solitude.* London: Faber and Faber Ltd.

Beaupre, G.S.; Orr, T.E.; Carter, D.R. 1990: An approach for time-dependent bone modeling and remodeling – Theoretical development. *J. Orthopaedic Res.*, 651–661

Bendsøe, M.P.; Kikuchi, N. 1988: Generating optimal topologies in structural design using a homogenization method. *Comp. Meth. Appl. Mech. Engrg.* **71**, 197–224

Diaz, A.; Bendsøe, M. 1992: Shape optimization of multipurpose structures by a homogenization method. *Struct. Optim.* **4**, 17–22

Dobbs, M.W.; Felton, L.P. 1969: Optimization of truss geometry. *J. Struct. Div., ASCE* **100**(ST1), 2105–1118

Dorn, W.C.; Gomory, R.E.; Greenberg, H.J. 1964: Automatic design of optimal structures. *J. de Mecanique* **3**, 25–52

Fuchs, M.B.; Paley, M.; Miroshnik, E. 1999: The Aboudi micromechanical model for shape design of structures. *Comp. Struct.* **73**, 355–362

Gibiansky, L.; Cherkaev, A. 1984: Design of composite plates of extremal rigidity. *Report 914*, Phys.-Tech. Inst., Acad. Sci. USSR, Leningrad English translation in: Cherkaev, A.; Kohn, R. (eds.) *Topics in the mathematical modeling of composite materials.* New York: Birkhauser, 1997

Haftka, R.T.; Gandhi, R.V. 1986: Structural shape optimization – A survey. *Comp. Meth. in Appl. Mech. and Eng.* **57**, 91–106

Haftka, R.T.; Gürdal, Z.; Kamat, M.P. 1990: *Elements of structural optimization.* Dordrecht: Kluwer

Hammer, V.B.; Olhoff, N. 1999: Topology optimization with design dependent loads. *WCSMO-3 Short Papers Proc.* (held in Buffalo), pp. 629–631

Herakovich, C.T. 1998: *Mechanics of fibrous material.* New York: John Wiley & Sons

Hinton, E.; Sienz, J. 1995: Fully stressed topological design of structures using an evolutionary approach. *Eng. Comput.* **12**, 229–244

Kirsch, U. 1989: Optimal topologies of Structures. *Appl. Mech. Rev.* **42**, 223–239

Kirsch, U. 1993: *Structural optimization.* Berlin, Heidelberg, New York: Springer

Lanyon, L.E. 1987: Functional strain in bone as an objective, and controlling stimulus for adaptive bone remodeling. *J. Biomech.* **20**, 1083–1093

Mattheck, C.; Burkhardt, S. 1990: A new method of structural shape optimization based on biological growth. *Int. J. Fatigue* **12**, 185–190

Maxwell, C. 1890: *Scientific papers II.* Cambridge: Cambridge University Press

Michell, A.G.M. 1904: The limits of economy of material in framed structures. *Phil. Mag.* **8**, 589–597

Olhoff, N.; Bendsøe, M.P.; Rasmussen, J. 1991: On CAD-integrated structural topology and design optimization. *Comp. Meth. Appl. Mech. Engrg.* **89**, 259–279

Olhoff, N.; Jacobson, J.B.; Rønholt, E. 1997: Three-dimensional structural topology and layout optimization based on optimum microstructures. *WCSMO-2 Second World Congress of Structural and Multidisciplinary Optimization, Extended Abstracts* (held in Zakopane), pp. 198–199

Rozvany, G.I.N.; Prager, W. 1979: A new class of structural optimization problems: optimal archgrids. *Comp. Meth. App. Mech. Engrg.* **19**, 49–58

Rozvany, G.I.N.; Bendsøe, M.P.; Kirsch, U. 1995: Layout optimization of structures. *Appl. Mech. Rev.* **48**, 41–119

Rozvany, G.I.N.; Wang, C.-M. 1983: On plane Prager-structures – I. *Int. J. Mech. Sci.* **25**, 519–527

Rozvany, G.I.N.; Wang, C.-M.; Dow, D. 1982: Prager–structures: archgrids and cable networks of optimal layout. *Comp. Meth. Appl. Mech. Engng.* **31**, 91–113

Rozvany, G.I.N.; Zhou, M.; Birker, T. 1992: Generalized shape optimization without homogenization. *Struct. Optim.* **4**, 250–252

Swanson Analysis Systems, Inc. 1992: *Ansys user's manual, Revision 5.0.* Houston

Suzuki, K.; Kikuchi, N. 1991: A homogenization method for shape and topology optimization. *Comp. Meth. Appl. Mech. Engng.* **93**, 291–318

Tanaka, M.; Adachi, T.; Tomita, Y. 1995: Optimum design of lattice continuum material suggested by mechanical adaptation model of cancellous bone. In: Olhoff, N.; Rozvany, G.I.N. (eds.) *WCSMO-1, Proc. First World Congress of Structural and Multidisciplinary Optimization* (held in Goslar, Germany), pp. 185–192. Oxford: Pergamon Press

Taylor J.E. 1977: Optimal truss design based on an algorithm using optimality criteria. *Int. J. Solids Struct.* **13**, 913–923

Van Keulen, F.; Hinton, E. 1996: Topology design of plate and shell structures using the hard kill method. In: *Advances in structural engineering optimization*, Civil-Comp Press, Edinburgh, pp. 167–176

Vigdergauz, S. 1986: Effective elastic parameters of a plate with a regular system of equal-strength holes. *Mech. Solids* **21**, 162–166

Xie, Y.M.; Steven, G.P. 1997: *Evolutionary structural optimization.* Berlin, Heidelberg, New York: Springer

Zhou, M.; Rozvany, G.I.N. 1991: The COC algorithm. Part II: Topological, geometrical and general shape optimization. *Comp. Meth. Appl. Mech. Eng.* **89**, 309–336